Thermoelectricity of clathrate I Si and Ge phases

2002 J. Phys.: Condens. Matter 14 7991

(http://iopscience.iop.org/0953-8984/14/34/318)

INSTITUTE OF PHYSICS PUBLISHING JOURNAL OF PHYSICS: CONDENSED MATTER

J. Phys.: Condens. Matter **14** (2002) 7991–8004 PII: S0953-8984(02)35727-8

Thermoelectricity of clathrate I Si and Ge phases

Ya Mudryk[1], P Rogl[1], C Paul[2], S Berger[2], E Bauer[2], G Hilscher[2], C Godart[3,4] and H Noël[5]

[1] Institut für Physikalische Chemie, Univ. Wien, Währingerstraße 42, A-1090 Wien, Austria
[2] Institut für Festkörperphysik, TU Wien, Wiedner Hauptstrasse 8-10, A-1040 Wien, Austria
[3] CNRS-UPR 209, ISCSA, 2-8 rue Henri Dunant, F94320 Thiais, France
[4] LURE-CNRS, Université Paris Sud, 91405 Orsay, France
[5] Laboratoire de Chimie du Solide et Inorganique Moléculaire, Université de Rennes I, UMR-CNRS 6511, Avenue du Général Leclerc, F-35042 Rennes Cedex, France

Received 10 April 2002, in final form 5 July 2002
Published 15 August 2002
Online at stacks.iop.org/JPhysCM/14/7991

Abstract

We report on investigations of type I clathrate Si and Ge compounds with Ba partially substituted by rare earth atoms. Novel compounds from framework-deficient solid solutions $Ba_8Al_xSi_{42-3/4x}\square_{4-1/4x}$ and $Ba_8Ga_xSi_{42-3/4x}\square_{4-1/4x}$ ($x = 8, 12, 16$; $\square$, open square... lattice defect) have been prepared and characterized. All x-ray intensity data are consistent with the standardized clathrate I-$Ba_8Al_{16}Ge_{30}$ type structure (space group $Pm\bar{3}n$). In rare earth substituted clathrates, $Eu_2Ba_6M_xSi_{46-x}$ (M = Cu, Al, Ga), rare earth atoms completely occupy the $2a$ position and thus form a new quaternary ordered version of the $Ba_8Al_{16}Ge_{30}$ structure type. From a geometrical analysis of clathrate crystal structures, a systematic scheme for all known clathrate compounds is proposed. All clathrates studied are metals with low electrical conductivity. The highest Seebeck coefficient in the present series is deduced for $Ba_8In_{16}Ge_{30}$, $S = -75\ \mu V\ K^{-1}$, indicating transport processes dominated by electrons as carriers. The Eu-based clathrates investigated exhibit long-range magnetic order as high as 32 K for $Eu_2Ba_6Al_8Si_{36}$ of presumably ferromagnetic type. Magnetic susceptibility indicates in all cases a 2+ ground state for the Eu ions, in fine agreement with L_{III} absorption edge spectra.

1. Introduction

Throughout recent years significant attention has been directed to a relatively new class of compounds: Ge- and Si-based, so-called clathrate phases with alkaline and earth alkaline metals [1]. The crystal structure of these compounds is characterized by an extended three-dimensional framework of germanium and silicon atoms providing huge voids usually filled by large electropositive elements such as in type I clathrates $M^I_8X^{IV}_{46}$ [2, 3] and in type II clathrates $M^I_xX^{IV}_{136}$ [4, 5] (M = Na, K, Rb; X = Si, Ge, Sn). Westerhaus and Schuster [6, 7] realized the stabilizing influence of X-atom/group-III element substitution in type I clathrates. These phases have cubic symmetry $Pm\bar{3}n$ or $P\bar{4}3n$. Whilst silicon

and germanium compounds $M^{II}_8B^{III}_{16}X^{IV}_{30}$ (M^{II} = Sr, Ba; B^{III} = Al, Ga, In; X^{IV} = Si, Ge) and $Ba_8M_8Ge_{38}$ (M = Zn, Cd, In) adopt the clathrate I structure, $Ba_8Ga_{16}Sn_{30}$ crystallizes with a new clathrate framework structure (clathrate type VIII; earlier called clathrate type III) [8, 9]. It was proposed that donor–acceptor interaction between alkaline and substituted atoms in the case of full electrical charge compensation might lead to a semiconducting state approaching the band structure of pure Ge [10]. Charge compensation may also be obtained by vacancy formation in the Ge sublattice and simple stoichiometric rules for the defect phases were proposed: $Ba_8Cd(Zn)_xGe_{42-1/2x}\square_{4-1/2x}$, $4 < x < 8$, and $Ba_8In_xGe_{42-3/4x}\square_{4-1/4x}$ with $4 < x < 16$, where $\square$ denotes a void in the germanium lattice. Clathrate frameworks stabilized by transition elements such as $Ba_8T_zX_{6-z}X_{40}$ (X = Ge, Si; T = Ni, Pd, Pt, Cu, Ag, Au) [11] yield a series of superconductors $Ba_8T_xSi_{46-x}$ (T = Cu, Ag, Au) [12] like $(Na, Ba)_8Si_{46}$ [13] and $Ba_8Ga_{16}Ge_{30}$ [14], whilst $Ba_8Mn_2Ge_{44}$ was found to be ferromagnetic at low temperature [15]. The main part of investigations performed on type I-clathrate compounds focused on their perspective thermoelectric properties. Nolas *et al* [16] reported absolute Seebeck coefficients approaching $-320\ \mu V\ K^{-1}$ for $Sr_8Ga_{16}Ge_{30}$; however, semiconducting properties of $Sr_8Ga_{16}Ge_{30}$ strongly depend on small deviations in composition (see also [17, 18]). For the best sample the figure of merit was $Z \sim 1.5 \times 10^{-3}\ K^{-1}$ at $T > 700$ K, comparable to $Ba_8Ga_{16}X_{30}$ (X = Si, Ge, Sn) [18]. Also system internal p-type thermoelectrics could be obtained, for example, $Ba_8Ga_{16}(GaSb)_xGe_{30-2x}$, $x \sim 2$, with $S = \sim 100\ \mu V\ K^{-1}$ [19]. First attempts to prepare europium-containing clathrates were successful for magnetic $Eu_8Ga_{16}Ge_{30}$ in which Eu atoms fill the guest sites [20–23]. A different type of covalent clathrate I, Ge-based semiconductors, $X_8A_8Ge_{38}$ (X = Cl, Br, I; A = P, As, Sb), with relatively high values of electrical resistivity (10^2–$10^9\ \Omega$ cm) was obtained by transport reactions [24].

Recently, $Ba_{24}Ge_{100}$ (Ba_6Ge_{25-x}) and isotypic phases $Ba_6Ge_{23}Sn_2$ and $Ba_6Ge_{22}In_3$ were described [25, 26] crystallizing in a new clathrate type derived from the clathrate I structure. A superstructure to type I clathrate was found in defect $Sn_{14}In_{10}P_{21.8}I_8$ [27]. Band structure calculations analysed with respect to structure stability conditions revealed that the large cage atoms form bonds with the whole cage rather than customary pair-wise interactions, whereas B^{III}-framework atoms avoid homonuclear bonds [28, 29].

The important feature of these materials with respect to their thermoelectric application is the cage structure providing a significant reduction of thermal conductivity when filled with big, heavy atoms rattling in the large void [30–33]. These cages may also be filled by rare-earth atoms particularly with intermediate valence behaviour creating additional possibilities for a decrease of thermal conductivity as well as for a modification of band structure.

Following these ideas, we report in this work on clathrate I, Si and Ge compounds with Ba partially substituted by Eu. Preparation conditions, crystal structure and physical properties considering possible thermoelectric application of these phases were studied.

2. Experimental details

Samples were prepared by argon arc melting of metal pieces of 99.9% minimum purity. To avoid Ba evaporation in the highly exothermic reaction a pre-calculated extra amount of Ba was added before melting: barium pieces were placed on top of the component mixture to prevent an unconditional intensive reaction process. Weight losses were less than 1.5 mass%. Usually, type I clathrate compounds formed after arc melting without annealing. However, in order to improve homogeneity, heat treatment was employed for all samples. $Ba_8Al_{16}Si_{30}$, $Ba_8Al_{12}Si_{33}$ and $Ba_8In_{16}Ge_{30}$ melt incongruently and were only obtained after annealing. Ge-containing samples were annealed in sealed quartz capsules for 10–14 days at 600 °C; Si samples were

Table 1. Lattice parameters of clathrate I compounds (space group $Pm\bar{3}n$).

Compound composition	Lattice parameter, a (nm)
$Ba_8Cu_6Si_{40}$	1.032 78(2)[a]
$Ba_8Cu_4Si_{42}$	1.032 66(4)
$Ba_8Cu_4Si_{38}Ga_4$	1.038 23(1)
$Ba_8Cu_4Si_{36}Ga_6$	1.040 38(5)
$Ba_8Cu_4Si_{34}Ga_8$	1.042 79(4)
$Ba_8Ga_8Si_{36}$	1.043 50(1)
$Ba_8Ga_{12}Si_{33}$	1.047 05(2)
$Ba_8Al_8Si_{36}$	1.048 90(1)
$Ba_8Al_{12}Si_{33}$	1.056 54(1)
$Ba_8Al_{16}Si_{30}$	1.062 85(1)[a]
$Eu_2Ba_6Cu_4Si_{42}$	1.030 53(2)
$Eu_2Ba_6Cu_4Si_{38}Ga_4$	1.036 41(5)
$Eu_2Ba_6Al_8Si_{36}$	1.049 51(2)
$Ba_8Al_{16}Ge_{30}$	1.085 18(1)[a]
$Ba_8In_{16}Ge_{30}$	1.121 77(1)[a]
$Ba_8Cu_4Ga_{20}Si_{22}$	1.050 89(6)
$Ba_8Ni_4Ga_{14}Ge_{28}$	1.077 98(2)

[a] For compounds already known in the literature, we present our lattice parameters.

annealed for 1–2 weeks at 850 °C (samples with high Ga content were annealed at 800 °C). After heat treatment all capsules were quenched in cold water. Most of the prepared samples were obtained as shiny solids quite stable in air, whilst $Ba_8Ni_4Ge_{42}$, $Ba_8Ga_{16}Ge_{30}$, $Ba_8Al_{16}Ge_{30}$ fragmented to powders within several hours. The resulting powder still represented the main phase without any traces of decomposition. Thus, we were led to assume that fragmentation was due to hydrolysis of impurities concentrated in low amounts on the grain boundaries. Attempts to synthesize iodine containing clathrates yielded single crystals of $I_8Sb_8Ge_{38}$, which were obtained by transport reactions, following the procedure described in [24].

Single-phase conditions of samples used for measurements of physical properties were assured from x-ray analyses employing x-ray Guinier image plate equipment at room temperature (flat powder specimen; range $8° \leqslant 2\theta \leqslant 100°$, step 0.005 in 2θ, Cu Kα1 radiation). Lattice parameters were calculated via a least squares routine using Si or Ge as calibration standards and are listed in table 1. Rietveld refinements of the samples were performed by use of the *FullProf98* program [34].

After single-crystal quality was assured from Weissenberg photographs, x-ray intensity data were collected on a four-circle Nonius Kappa diffractometer equipped with a CCD area detector employing graphite monochromated Mo Kα radiation ($\lambda = 0.071\,073$ nm). The distance between crystal and detector was 25 mm. Orientation matrix and unit cell parameters were derived from the first ten frames using the program DENZO [35]. Absorption correction was taken from program SORTAV [35]. The structure was refined employing the SHELXS-97 program [36]. Experimental parameters and results of structure refinement are listed in tables 3 and 4.

Bulk properties (temperature dependent resistivity, temperature dependent thermal conductivity and thermopower as well as x-ray absorption spectroscopy, magnetic susceptibility and specific heat) were obtained by a variety of standard techniques, described in detail in [37].

Table 2. X-ray powder diffraction refinement data for $Ba_8In_{16}Ge_{30}$ and $Ba_8Ga_{12}Si_{33}$.

Parameter	$Ba_8In_{16}Ge_{30}$	$Ba_8Ga_{12}Si_{33}$
Structure type	$Ba_8Al_{16}Ge_{30}$	$Ba_8Al_{16}Ge_{30}$
Space group	$Pm\overline{3}n$	$Pm\overline{3}n$
a (nm)	1.121 77(1)	1.048 61(2)
V (nm^3)	1.411	1.1530
ρ_x (M gm^{-3})	6.056	4.118
2θ range	15°–100°	15°–100°
Reflections measured	148	125
Number of variables	26	28
$R_F = \Sigma\|F_0 - F_c\|/\Sigma F_0$	0.085	0.058
$R_I = \Sigma\|I_{0B} - I_{cB}\|/\Sigma I_{0B}$	0.099	0.101
$R_{wP} = [\Sigma w_i\|y_{0i} - y_{ci}\|^2/\Sigma w_i\|y_{0i}\|^2]^{1/2}$	0.107	0.091
$R_P = \Sigma\|y_{0i} - y_{ci}\|/\Sigma\|y_{0i}\|$	0.076	0.065
$R_e = [(N - P + C)/(\Sigma w_i y_{0i}^2)]^{1/2}$	0.039	0.031
$\chi^2 = (R_{wP}/R_e)^2$	7.67	8.78
Calculated composition	$Ba_8In_{16.87}Ge_{29.13}$	$Ba_8Ga_{11.5}Si_{33.2}$
Atomic parameters		
Ba1	2*a*(0 0 0)	2*a*(0 0 0)
B_{iso} 10^2 (nm^2)	0.98(5)	1.71(3)
Occ.	1	1
Ba2	6*c*(1/4 0 1/2)	6*c*(1/4 0 1/2)
B_{iso} 10^2 (nm^2)	3.8(1)	3.00(3)
Occ.	1	1
M1	6*d*(1/4 1/2 0)	6*d*(1/4 1/2 0)
B_{iso} 10^2 (nm^2)	2.20(5)	1.75(5)
Occ.	0.75(1)In + 0.25Ge	0.80(1)Ga + 0.20Si
M2	16*i*(0.185 06(7) *xx*)	16*i*(0.1838(1) *xx*)
B_{iso} 10^2 (nm^2)	1.85(3)	1.65(5)
Occ.	0.20(2)In + 0.80Ge	0.97(1)Si
M3	24*k*(0 0.116 39(7) 0.305 71(7))	24*k*(0 0.1195(1) 0.3064(1))
B_{iso} 10^2 (nm^2)	1.91(3)	1.50(3)
Occ.	0.38(2)In + 0.62Ge	0.73(1)Si + 0.27Ga

3. Results

3.1. Compound formation and structural chemistry

X-ray intensity patterns of all clathrate compounds prepared were indexed on the basis of the standardized clathrate I-$Ba_8Al_{16}Ge_{30}$ type structure with space group $Pm\overline{3}n$ [38]. Rietveld refinement and single-crystal studies did not reveal any significant deviation from centrosymmetry as for instance claimed for $Na_8(Al, Ge)_{46}$ with space group $P\overline{4}3n$ [7]. Results of Rietveld refinements and single-crystal studies are summarized in tables 2–4.

3.1.1. Rare earth substituted compounds. Substitution of Ba by rare earth metal such as Eu seems to have a stabilizing effect: single-crystal x-ray data in all cases reveal full atomic order among Eu and Ba atoms. The rare earth atoms thereby tend to occupy the smaller voids in the Si framework (Eu in sites 2*a*, Ba in sites 6*c*) and thus form a new quaternary ordered version of the $Ba_8Al_{16}Ge_{30}$ structure type.

Table 3. X-ray single-crystal data for $Eu_2Ba_6Cu_4Si_{42}$ and $Eu_2Ba_6Al_8Si_{36}$ clathrates ($Ba_4Al_8Ge_{15}$ type, space group $Pm\bar{3}n$; no 223, origin at centre) and interatomic distances.

Parameter	$Eu_2Ba_6Cu_4Si_{42}$	$Eu_2Ba_6Al_8Si_{36}$
Crystal size	$50 \times 28 \times 56$ μm^3	$70 \times 42 \times 56$ μm^3
a (nm)	1.030 68(2)	1.049 51(2)
ρ_x (Mg cm^{-3})	3.885	3.383
μ_{abs} (mm^{-1})	11.18	8.80
Data collection, 2Θ range (deg)	$2 \leqslant 2\Theta \leqslant 74$; 120 s/frame	$2 \leqslant 2\Theta \leqslant 70$; 60 s/frame
Total number of frames	205	205
Reflections in refinement	$390 \leqslant 4\sigma$(Fo) of 528	$398 \leqslant 4\sigma$(Fo) of 487
Mosaicity	<0.52	<0.56
Number of variables	16	18
$R_F^2 = \Sigma\lvert F_0^2 - F_c^2\rvert / \Sigma F_0^2$	0.034	0.034
R_{Int}	0.068	0.069
wR2	0.112	0.086
GOF	1.137	1.135
Extinction (Zachariasen)	0.002 99(6)	0.001 24(3)
Eu in 2a(0,0,0); occ.	**2Eu**, 1.00(1)	**2Eu**, 1.00(1)
$U_{11} = U_{22} = U_{33}$	0.0166(2)	0.0166(2)
Ba in 6c(1/4, 0, 1/2); occ.	**6Ba**, 1.00(1)	**6Ba**, 1.00(1)
$U_{11} = U_{22}$, U_{33}	0.0331(3), 0.0200(3)	0.0242(2), 0.0163(3)
Cu(Al1) in 6d(1/4, 1/2, 0); occ.	**4.00(1) Cu + 2 Si**, 1.00(1)	**6Al1**, 1.00(1)
$U_{11} = U_{22}$, U_{33}	0.0136(6), 0.0120(4)	0.0083(11), 0.0102(7)
Si1(M) in 16i(x, x, x); occ.	**24Si**, $x = 0.183\,98(9)$; 1.00(1)	**14.00(1) Si1 + 2 Al2**, $x = 0.184\,48(9)$; 1.00(1)
$U_{11} = U_{22} = U_{33}$	0.0110(3)	0.0127(5)
Si2 in 24k(0, y, z); occ.	**24Si**, $y = 0.1193(1)$; $z = 0.3088(1)$; 1.00(1)	**24Si**, $y = 0.1158(1)$; $z = 0.3029(1)$; 1.00(1)
U_{11}, U_{22}, U_{33}	0.0127(5), 0.0125(5), 0.0108(5)	0.0134(6), 0.0116(6), 0.0134(6)
Residual density; max; min	1.61; −4.49	1.34; −3.25
Principal mean square atomic displacements U	Eu 0.0166 0.0166 0.0166 Ba 0.0330 0.0330 0.0200 Cu 0.0136 0.0120 0.0120 Si3 0.0117 0.0117 0.0096 Si2 0.0129 0.0123 0.0108	Eu 0.0166 0.0166 0.0166 Ba 0.0243 0.0243 0.0162 Al1 0.0102 0.0102 0.0083 M1 0.0135 0.0135 0.0112 Si2 0.0139 0.0134 0.0111

Interatomic distances

Central atom	Ligand	Distance (nm)	Ligand	Distance (nm)
Eu	−8Si1	0.328 4(2)	−8M	0.335 3(2)
	−12Si2	0.341 2(1)	−12Si	0.340 4(1)
Ba	−8Si2	0.346 90(8)	−8Si	0.355 51(9)
	−4Cu	0.364 4(1)	−4Al1	0.371 06(9)
Cu (Al)	−4Si2	0.238 7(1)	−4Si	0.250 3(1)
	−4Ba	0.364 4(1)	−4Ba	0.371 06(9)
Si1 (M)	−1Si1	0.235 7(3)	−1M	0.238 2(3)
	−3Si2	0.238 66(9)	−3Si	0.241 1(1)
	−1Eu	0.328 4(1)	−1Eu	0.335 3(2)
Si2	−2Si1	0.238 66(9)	−2M	0.241 1(2)
	−1Cu	0.238 7(1)	−1Si	0.242 0(3)
	−1Si2	0.245 9(3)	−1Al1	0.250 3(1)
	−1Eu	0.341 2(1)	−1Eu	0.340 4(1)
	−2Ba	0.346 90(8)	−2Ba	0.355 51(9)

Table 4. X-ray single-crystal data for $I_8Sb_8Ge_{38}$ clathrate ($Ba_4Al_8Ge_{15}$ type, space group $Pm\bar{3}n$; no 223, origin at centre) and interatomic distances.

Parameter	$I_8Sb_8Ge_{38}$
Crystal size	$28 \times 30 \times 90\ \mu m^3$
a (nm)	1.087 90(3)
ρ_x (Mg cm^{-3})	6.123
μ_{abs} (mm^{-1})	30.70
Data collection, 2Θ range (°)	$2 \leqslant 2\Theta \leqslant 72.6$; 40 s/frame
Total number of frames	201
Reflections in refinement	$531 \leqslant 4\sigma$(Fo) of 592
Mosaicity	<0.44
Number of variables	22
$R_F^2 = \Sigma\lvert F_0^2 - F_c^2\rvert / \Sigma F_0^2$	0.0375
R_{Int}	0.068
wR2	0.102
GOF	1.155
Extinction (Zachariasen)	0.0023(2)
I1 in 2*a*(0,0,0); occ.	**2I1**, 1.00(1)
$U_{11} = U_{22} = U_{33}$	0.0138(3)
I2 in 6*c*(1/4, 0, 1/2); occ.	1.00(1) **I2**
$U_{11} = U_{22}$, U_{33}	0.0199(3), 0.0109(4)
M1 in 6*d*(1/4, 1/2, 0); occ.	**5.2(1) Ge1 + 0.8 Sb1**, 1.00(1)
$U_{11} = U_{22}$, U_{33}	0.0178(7), 0.0126(5)
M2 in 16*i*(x, x, x); occ.	**12.5(1) Ge2 + 3.5 Sb2**, $x = 0.183\,62(4)$; 1.00(1)
$U_{11} = U_{22} = U_{33}$	0.0116(2)
M3 in 24*k*(0, y, z); occ.	**20.36(2) Ge3 + 3.64 Sb3**, $y = 0.117\,32(7)$; $z = 0.308\,86(7)$; 1.00(1)
U_{11}, U_{22}, U_{33}	0.0135(3), 0.0143(3), 0.0142(3)
Residual density; max; min	1.67; −3.62
Principal mean square atomic displacements U	I1 0.0138 0.0138 0.0138 I2 0.0199 0.0199 0.0109 Ge1 0.0178 0.0126 0.0126 Ge2 0.0117 0.0117 0.0114 Ge3 0.0155 0.0142 0.0123

Central atom	Ligand	Distance (nm)
I1	−8M2	0.345 99(5)
	−12M3	0.359 43(8)
I2	−8M3	0.365 38(6)
	−4M1	0.384 63(3)
M1	−4M3	0.253 13(7)
	−4I2	0.384 63(3)
M2	−1M2	0.250 2(2)
	−3M3	0.252 33(5)
	−1I1	0.345 99(5)
M3	−2M2	0.252 33(5)
	−1M1	0.253 13(7)
	−1M3	0.255 2(1)
	−1I1	0.359 43(8)
	−2I2	0.365 38(6)

Although we are not able to distinguish between Si and Al atoms due to only a difference of one electron resulting in similar x-ray scattering power, the significantly longer interatomic distances point to the fact that Al occupies the 6*d* position. Even in single-crystal data

sensitivity is not high enough to locate stoichiometric defects and all framework positions generally tend to show full occupation. This is particularly intriguing for $Eu_2Ba_6Al_8Si_{36}$ for which single-crystal refinements yield practically full occupation of framework positions, but a sample '$Eu_2Ba_6Al_8Si_{38}$' was not obtained as a single phase. This confirms that defects, probably distributed over the whole Si/Ge-framework, are important for structure stabilization.

In contrast to the proposition in the literature [24], our crystal structure refinement for $I_8Sb_8Ge_{38}$ arrived at lowest residual values for the centrosymmetric space group $Pm\overline{3}n$. There are no deviations requesting the loss of the centre of symmetry (space group $P\overline{4}3n$ and lower), and furthermore there are no indications for Sb/Ge ordering either in $Pm\overline{3}n$ or in lower symmetry space groups such as $P\overline{4}3n$, $P\overline{4}3$, $Pm\overline{3}$ or $P23$. Iodine atoms adopt the alkaline earth atom positions; thus the entire atom arrangement resembles a typical clathrate I structure.

3.1.2. Compounds with framework substitution. Similar to the $Ba_8In_xGe_{42-3/4x}\square_{4-1/4x}$ series reported in [10], novel compounds from three solid solutions were prepared: $Ba_8Cu_4Si_{42-x}Ga_x$ ($x = 0, 4, 6, 8$), $Ba_8Al_xSi_{42-3/4x}\square_{4-1/4x}$ and $Ba_8Ga_xSi_{42-3/4x}\square_{4-1/4x}$ ($x = 8, 12, 16$; $\square$—lattice defect). The latter two series use framework defects in addition to group III element substitution for charge compensation. In all cases, lattice parameters linearly increase with decreasing silicon content, i.e. with increasing content of the large group III element (see table 1).

As a convention, all prepared compounds can be divided into two groups:

(1) 'Cordier' phases $Ba_8T_xGe(Si)_{46-x}$ (T = Ni, Pd, Pt, Au, Cu, Ag) in which only the 6*d* framework site is occupied by metal atoms
(2) compounds which may exhibit framework deficiency subject to certain stoichiometry rules, described in [10].

In a successful attempt to combine these two types, we obtained compounds of intermediate position between types (1) and (2), such as $Ba_8Ni_4Ga_{14}Ge_{28}$ and $Ba_8Cu_4Si_{36}Ga_6$. Probably, the formation conditions of both of these types are similar—in 'Cordier' phases the electroneutrality point approaches by substitution of group IV atoms like Si/Ga in $Ba_8Ga_8Si_{36}\square_2$, but voids are filled by transition metal atoms.

The analysis of interatomic distances (tables 3, 4) in clathrate compounds reveals interesting features: distances among framework atoms (Si, Ge and substituted atoms) are significantly decreased in comparison to the sum of their atomic radii. This fact can be explained by the covalent origin of interatomic bonds. In contrast, distances between these atoms and Ba (Eu) situated in the large voids are much longer and point towards a weak interaction between host atoms and main framework. These weak bonds are responsible for the rattling mode of the large barium and europium atoms as already anticipated in [17, 20, 33].

3.1.3. Scheme of clathrate structure types. Although many papers deal with the crystal structure of clathrate materials, Fukuoka *et al* [25] revealed structure relations between clathrate I and II phases and the new Ba_6Ge_{25} type, identifying the pentagonal dodecahedron $BaGe_{20}$ as the fundamental structural unit. All these clathrates belong to the cubic system with different ways of packing the Ge_{20} dodecahedra. The Ba_6Ge_{25} structure derives from clathrate I with Ge_{20} dodecahedra and Ge_{20} open cages formed by removal of four germanium atoms. Consequently a new Ba-filled structural unit $BaGe_8$ is formed.

In contrast to the clathrate I type, where Ge_{20} dodecahedral units are isolated and mutually connected through face-sharing Ge_{24} tetrakaidecahedra, these units are in direct contact for

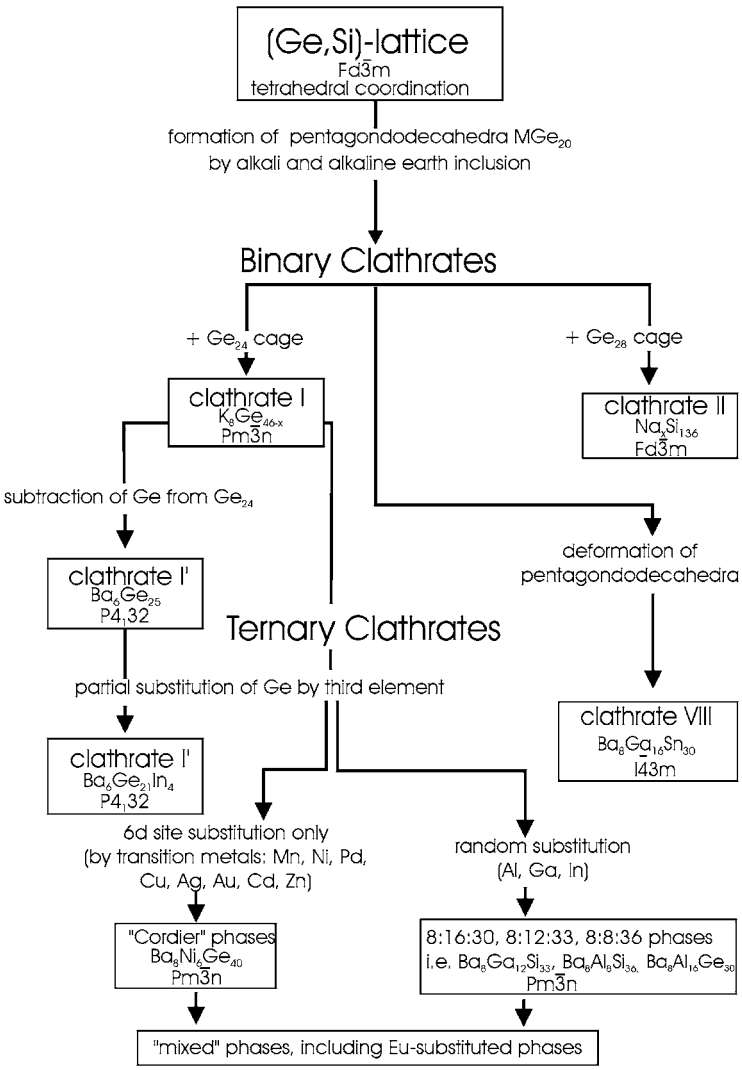

Figure 1. Relationships between different clathrate structure types—clathrate structure family tree. Sn-containing phases exhibit various superstructures not listed here. *Earlier called clathrate III.

the clathrate II type. The layers of Ge_{20} in this case are packed along the threefold cubic axis with larger Ge_{28} cages situated between the layers [4]. In the clathrate VIII structure ($Ba_8Ga_{16}Sn_{30}$-type) [8] pentagonal faces of Ge_{20} polyhedra are deformed and 'split' into triangles and trapeziums.

Taking into account the conventional framework packing mode in all the known clathrate compounds we propose a novel scheme as a clathrate structure family tree shown in figure 1. The original Ge (Si) lattice is taken as the starting point; all clathrate atoms with tetrahedral coordination form the main framework even in the case of In or Sb substitution. Ba_6Ge_{25}, as a simple derivative from the clathrate I structure, is labelled 'clathrate I'[6].

[6] Alternatively, Ba_6Ge_{25} may be labelled as clathrate IX.

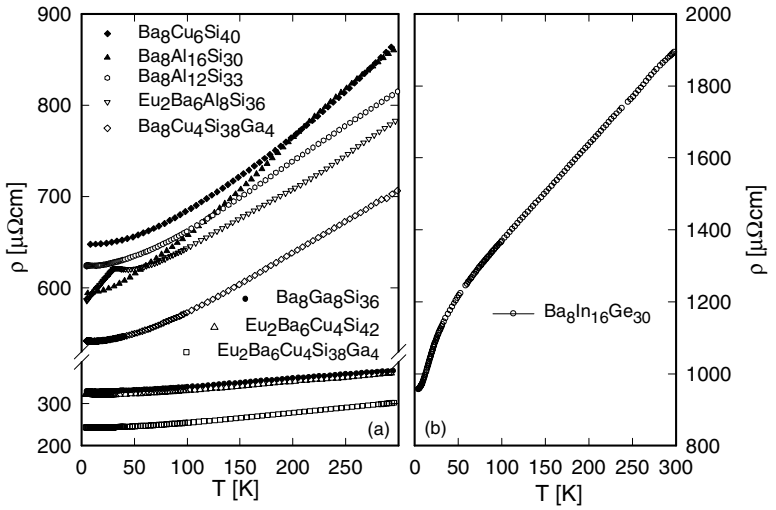

Figure 2. (a), (b) Temperature dependent resistivity ρ for selected clathrates.

3.2. Physical properties

3.2.1. Electrical resistivity. The temperature dependent electrical resistivity $\rho(T)$ of selected materials is summarized in figures 2(a) and (b), revealing generally metallic features. From the overall shape of $\rho(T)$ one easily distinguishes two classes of behaviour:

(i) Eu free samples obey the Bloch–Grüneisen relation in the full range of measured temperatures and least squares fits yield Debye temperatures of about 300 K in accordance with a rigid framework of essentially covalent bonds. In this context, the significantly lower Debye temperature (100–200 K) of ternary filled skutterudites [39] is in line with the softened $CoAs_3$-type framework.

(ii) Eu containing samples are characterized by additional spin dependent scattering processes, giving rise to further low temperature resistivity features. In particular, $Eu_2Ba_6Al_8Si_{36}$ exhibits long range magnetic order below 32 K as obvious from a pronounced cusp in $\rho(T)$, confirmed by susceptibility and specific heat data. Both compounds $Eu_2Ba_6Cu_4Si_{42}$ and $Eu_2Ba_6Cu_4Si_{38}Ga_4$ also show magnetic order, however at temperatures as low as 5 and 4 K, respectively (see below).

$Ba_8In_{16}Ge_{30}$ with a rather high absolute resistivity behaves differently. Although the system does not contain any magnetic scatterers, the overall resistivity significantly deviates from the Bloch–Grüneisen law associated with simple metallic conductivity. In particular, the strong curvature around 30 K resembles a behaviour frequently found in strongly correlated electron systems.

In order to prove local magnetism in the magnetically ordered compound $Eu_2Ba_6Al_8Si_{36}$, resistivity was studied under pressure up to 16 kbar (see figures 3(a) and (b)). Two main features become apparent: (i) a significant overall decrease of resistivity and (ii) an increase of the magnetic ordering temperature upon pressure at an initial rate of about 0.22 K kbar^{-1}. Some irregular change of $\rho(T, p)$ under pressure is referred to the brittleness of the sample. The increase of T_{mag} can be considered as a typical sign for well localized magnetic moments consistent with the Eu^{2+} ground state, yielding a total angular momentum $J = 7/2$. The shallow minimum in $\rho(T)$ located slightly above the ordering temperature would be in line

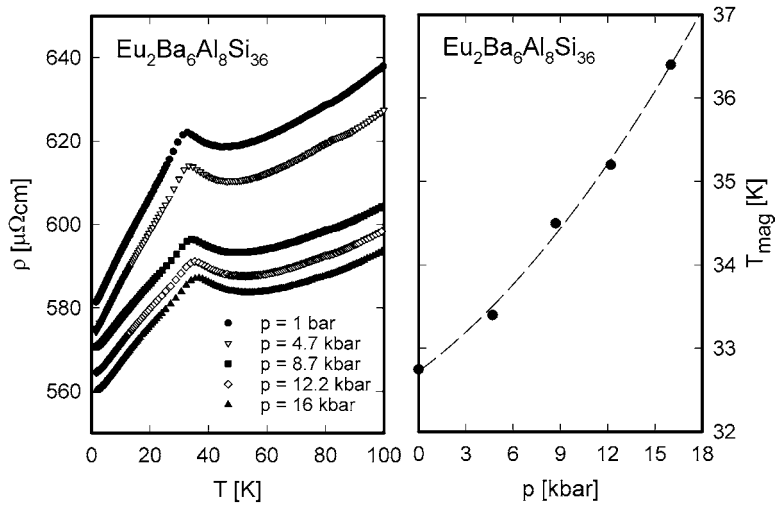

Figure 3. (a) Temperature dependent resistivity ρ of $Eu_2Ba_6Al_8Si_{36}$ for various values of applied pressure. (b) Pressure dependence of magnetic transition as a function of pressure for $Eu_2Ba_6Al_8Si_{36}$.

with a ferromagnetic ground state: associated ferromagnetic fluctuations persisting above the ordering temperature cause the observed rise of $\rho(T)$. Magnetoresistance of the Eu based samples, studied in fields up to 12 T, was negative in all cases and remained within 1% below 40 K. Ferromagnetic order and spin fluctuations slightly above the respective ordering temperature agree with the negative magnetoresistance observed.

3.2.2. Magnetism. The ferromagnetic type of order is reflected from magnetization and susceptibility data (figures 4(a) and (b)). Isothermal magnetization versus field shows spontaneous magnetization, without full saturation at the maximum field of 6 T. The maximum values of about 5.5 μB per europium atom, as obtained for the 2 K curves for the Eu based compounds at 6 T, are well below the expected magnetization associated with a simple collinear Eu^{2+} ferromagnet. Such behaviour may indicate a more complicated Eu-spin arrangement, or a ferrimagnetic type of ordering. Arrott plots of M/H versus H^2 in conjunction with $\chi_{a.c.}$ give ordering temperatures of 32, 5 and 4 K, for $Eu_2Ba_6Al_8Si_{36}$, $Eu_2Ba_6Cu_4Si_{42}$ and $Eu_2Ba_6Cu_4Si_{38}Ga_4$, respectively. Analysing the inverse magnetic susceptibility $1/\chi(T)$ above about 50 K in terms of the modified Curie–Weiss law (see figure 4(a)) yields positive paramagnetic Curie temperatures (19.6, 5.5 and 9.7 K, listed in the sequence given above), indicating a ferromagnetic type of interaction. The deduced Curie constant reveals effective magnetic moments for Eu per formula unit of 7.82, 8.02 and 7.53 μB, respectively, close to the ideal divalent Eu[$\mu_{eff}(Eu^{2+}) = 7.94\ \mu_B$]. Slightly lower values may arise for two reasons, i.e. small Eu defects in the 2*a* sites and/or from a slight shift of the Eu valence towards non-magnetic Eu^{3+}. However, a proof of almost perfect divalency of Eu in Eu based clathrates is obvious from the L_{III} absorption edge measurements performed at $T = 300$ and 10 K as shown in figure 5. Applying a standard deconvolution technique [39], already used in previous studies of Eu compounds, reveals divalency of Eu, nearly independent of temperature. These data are therefore in agreement with the appearance of magnetic order.

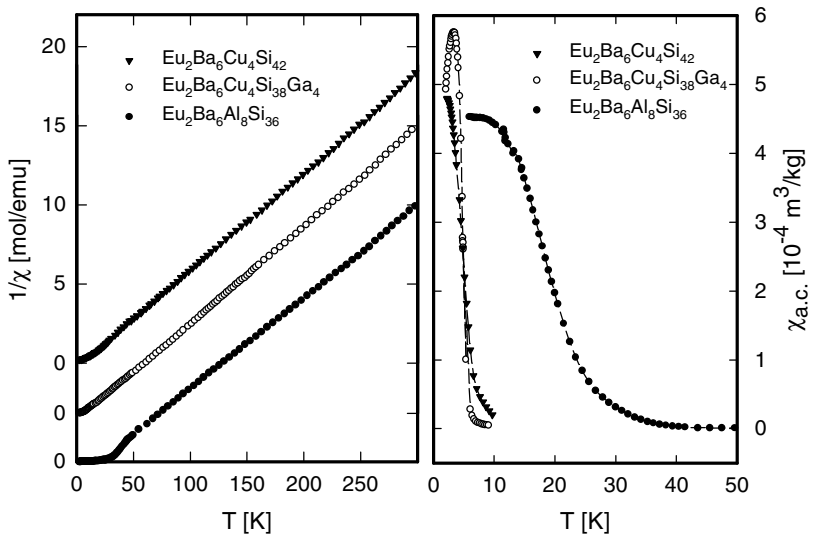

Figure 4. (a) Temperature dependent inverse magnetic susceptibility $1/\chi$ of $Eu_2Ba_6Cu_4Si_{38}Ga_4$, $Eu_2Ba_6Cu_4Si_{42}$ and $Eu_2Ba_6Al_8Si_{36}$. (b) Temperature dependent $\chi_{a.c.}$ for clathrates in (a); data for $Eu_2Ba_6Cu_4Si_{38}Ga_4$ were divided by a factor of two.

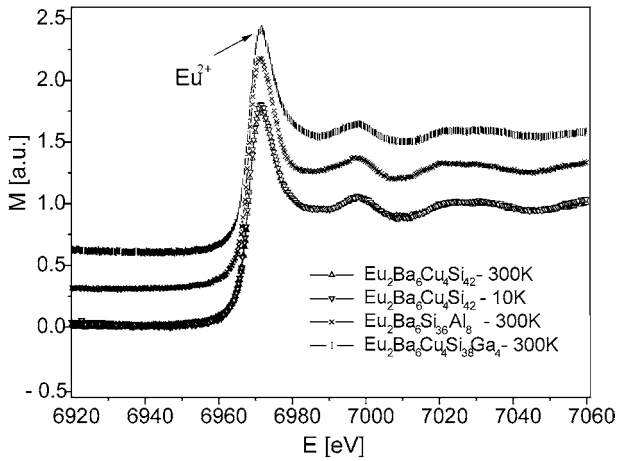

Figure 5. Energy dependent L_{III} absorption edge of Eu substituted clathrates.

3.2.3. Seebeck effect. Figures 6(a) and (b) summarize the temperature dependent Seebeck coefficient S for selected clathrates. At elevated temperatures $S(T)$ behaves almost linearly and exhibits negative sign. The largest absolute value at room temperature is deduced for $Ba_8In_{16}Ge_{30}$ with about $-75\ \mu V\ K^{-1}$. Large values of the Seebeck effect are usually associated with a low carrier density, which in turn corresponds to high resistivity values. In fact $Ba_8In_{16}Ge_{30}$ exhibits the largest $\rho(T)$ values throughout our materials studied (compare figure 2(a)). Moreover, negative values of the Seebeck coefficient are in line with electrons as essential charge carriers in the system. The nearly linear dependence of $S(T)$ at elevated temperatures excludes strong electron interactions. Figure 6(b) shows $S(T)$ of the Eu based clathrates in more detail. It is interesting to note the sequence of the compounds

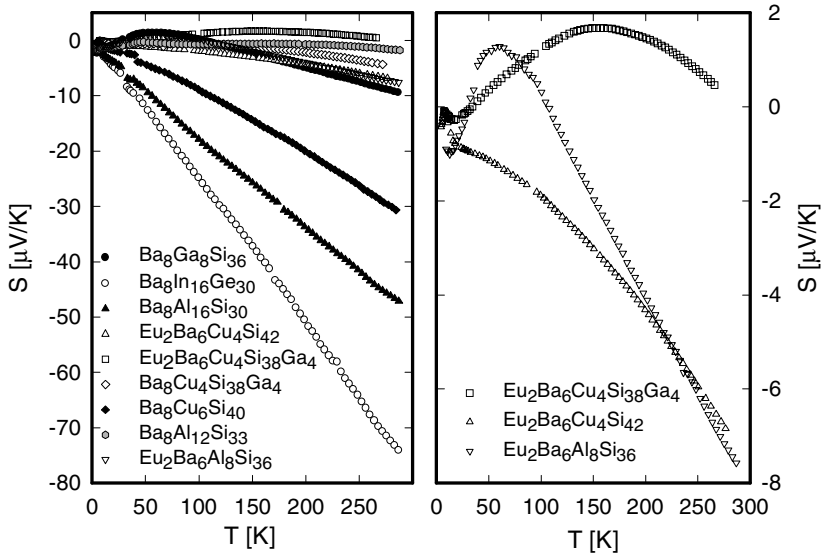

Figure 6. (a) Temperature dependent thermopower S of selected clathrate compounds. (b) $S(T)$ of $Eu_2Ba_6Cu_4Si_{38}Ga_4$, $Eu_2Ba_6Cu_4Si_{42}$ and $Eu_2Ba_6Al_8Si_{36}$.

$Eu_2Ba_6Cu_4Si_{38}Ga_4$, $Eu_2Ba_6Al_8Si_{36}$ and $Eu_2Ba_6Cu_4Si_{42}$, with a change from predominantly positive $S(T)$ values to negative $S(T)$. The relatively small values found for the Eu based compounds may hint at a larger number of carriers, in agreement with the best conducting samples of the series. In best accordance with the electron count, the sign of the Seebeck effect classifies $Eu_2Ba_6Cu_4Si_{38}Ga_4$ as a hole dominated carrier system, whilst $Eu_2Ba_6Cu_4Si_{42}$ is an electron dominated system (as in a semiconductor, the Si/Ga substitution is assumed to subtract one electron per atom).

3.2.4. Thermal conductivity and figure of merit. The temperature dependent thermal conductivity $\lambda(T)$ was measured for $Ba_8Al_{16}Si_{30}$ and is displayed in figure 7. $\lambda(T)$ exhibits a maximum around 11 K with comparatively large values of about 66 mW cm^{-1} K^{-1}. The relatively strong rise above about 220 K may originate, at least partly, from radiation losses of the sample. A comparison with typical intermetallics, however, reveals a significantly reduced thermal conductivity of $Ba_8Al_{16}Si_{30}$, in good accordance with novel skutterudites. The main reason for the observed low $\lambda(T)$ values is associated with a strong interplay of the heat carrying lattice vibrations with the loosely bound electropositive elements in the large voids of the cage structure. The measured total thermal conductivity λ can be expressed as $\lambda = \lambda_e + \lambda_{ph}$ where λ_e represents the electronic part and λ_{ph} the lattice contribution. Both λ_e and λ_{ph} are constrained by a number of scattering processes, responsible for a finite thermal resistivity. Assuming the validity of the Wiedemann–Franz law $\lambda_e = L_0 T/\rho$, where $L_0 = 2.45 \times 10^{-8}$ W Ω^{-1} K^{-2} is the Lorenz number (derived in the scope of the free electron model) and ρ is the electrical resistivity of the sample, λ_e and λ_{ph} can be separated from the total measured effect. Results of such a procedure are shown as dashed and dash–dotted curves for λ_{ph} and λ_e, respectively. Although such an analysis can give just a crude approximation, it evidences that heat in this compound is primarily carried by the phonon system while the electronic part is very small, in line with the relatively high electrical resistivity due to a reduced number of free carriers. According to the Seebeck effect, electrons are the principal carriers in $Ba_8Al_{16}Si_{30}$.

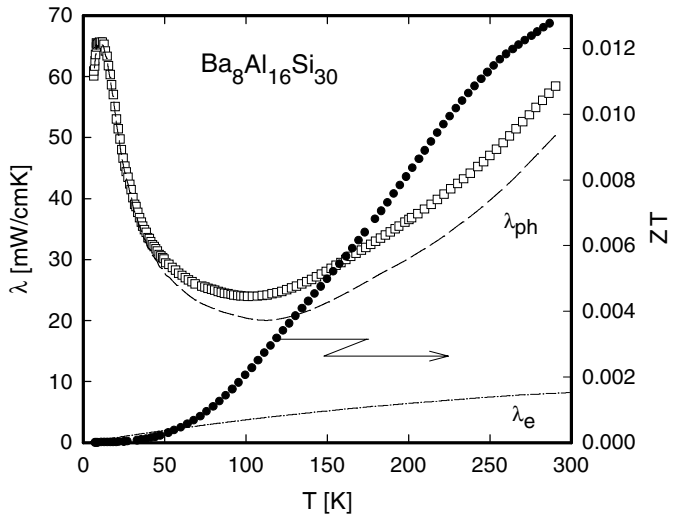

Figure 7. Left axis: temperature dependent thermal conductivity λ of $Ba_8Al_{16}Si_{30}$. The dashed and the dashed–dotted curves are the phonon and the lattice contribution to $\lambda(T)$, respectively. Right axis: figure of merit ZT of $Ba_8Al_{16}Si_{30}$.

The figure of merit $ZT = S^2/(\rho\lambda)$ derived for $Ba_8Al_{16}Si_{30}$ (right axis, figure 7) keeps low over the whole temperature range studied, mainly because $S(T)$ stays below 100 μV K^{-1}.

4. Summary

A series of Ba and rare earth (Eu) substituted clathrates of type I (space group $Pm\overline{3}n$) was synthesized including Cu-stabilized variants with various substitutions within the Si (Ge) framework by Al, Ga or In atoms or vacancies. Based on single-crystal x-ray studies, rare earth atoms were found to occupy the 2*a* position and thus form a new quaternary ordered version of the $Ba_4Al_8Ge_{15}$ structure type. From an analysis of the geometry and symmetry of crystal structures involved, a systematic scheme for all known clathrate compounds is proposed. The temperature dependent electrical resistivity characterizes all the clathrates studied as metals with low conductivity. The Eu based clathrates exhibit long range magnetic order as high as 32 K for $Eu_2Ba_6Al_8Si_{36}$ of presumably ferromagnetic type. Magnetic susceptibility indicates an almost 2+ state for the Eu ions, in fine agreement with L_{III} absorption edge spectra.

With a Seebeck coefficient of -75 μV K^{-1}, $Ba_8In_{16}Ge_{30}$ is a perspective thermoelectric material, indicating transport processes dominated by electrons as carriers. To a lower degree this also holds for $Ba_8Al_{16}Si_{30}$ and $Ba_8Cu_6Si_{40}$.

Acknowledgments

This research was sponsored by the Austrian FWF under grant P12899 and P13778 as well as by a grant for an international joint research project NEDO (Japan). The authors are grateful to the OEAD for support within the framework of the Austrian–French bilateral exchange program Amadee, project V.9.

References

[1] Pauling L and Marsh R 1952 *Proc. Natl Acad. Sci. USA* **38** 112
[2] Gallmeier J, Schäfer H and Weiss A 1969 *Z. Naturf.* b **24** 665
[3] Kaspar J S, Hagenmuller P, Pouchard M and Cros C 1965 *Science* **150** 1713
[4] Cros C, Pouchard M and Hagenmuller P 1970 *J. Solid State Chem.* **2** 570
[5] Nolas G S, Ward J-M, Gryko J, Qiu L and White M A 2001 *Phys. Rev.* B **64** 153201
[6] Schuster H-U and Westerhaus W 1975 *Z. Naturf.* b **30** 805
[7] Westerhaus W and Schuster H-U 1977 *Z. Naturf.* b **32** 1365
[8] Eisenmann B, Schäfer H and Zagler R 1986 *J. Less-Common. Met.* **118** 43
[9] Czybulka A, Kuhl B and Schuster H-U 1991 *Z. Anorg. Allg. Chem.* **594** 23
[10] Kuhl B, Czybulka A and Schuster H-U 1995 *Z. Anorg. Allg. Chem.* **621** 1
[11] Cordier G and Woll P 1991 *J. Less-Common Met.* **169** 291
[12] Herrmann R F W, Tanigaki K, Kuroshima S and Suematsu H 1998 *Chem. Phys. Lett.* **283** 29
[13] Yamanaka S, Horie H-O, Kawaji H and Ishikawa M 1995 *Eur. J. Solid State Inorg. Chem.* **32** 799
[14] Bryan J D, Srdanov V I, Stucky G D and Schmidt D 1999 *Phys. Rev.* B **60** 3064
[15] Kawaguchi T, Tanigaki K and Yasukawa M 2000 *Appl. Phys. Lett.* **77** 3438
[16] Nolas G S, Cohn J L, Slack G A and Schujman S B 1998 *Appl. Phys. Lett.* **73** 178
[17] Blake N P, Mollnitz L, Kresse G and Metiu H 1999 *J. Chem. Phys.* **111** 3133
[18] Schujman S B, Nolas G S, Young R A, Ling C, Wilkinson A P, Slack G A, Patschke R, Kanatzidis M G, Ulutagay M and Hwu S-J 2000 *J. Appl. Phys.* **87** 1529
[19] Latturner S, Bu X, Blake N, Metiu H and Stucky G 2000 *J. Solid State Chem.* **151** 61
[20] Cohn J L, Nolas G S, Fessatidis V, Metcalf T H and Slack G A 1999 *Phys. Rev. Lett.* **82** 779
[21] Pacheco V, Bentien A, Carrillo-Cabrera W, Paschen S, Steglich F and Grin Y 2001 *ECSSC8 (Oslo)* P092 (Abstracts)
[22] Chakoumakos B C, Sales B C and Mandrus D G 2001 *J. Alloys Compounds* **322** 127
[23] Sales B C, Chakoumakos B C, Jin R, Thompson J R and Mandrus D 2001 *Phys. Rev.* B **63** 245113
[24] Menke H and von Schnering H G 1973 *Z. Anorg. Allg. Chem.* **395** 223
[25] Fukuoka H, Iwai K, Yamanaka S, Abe H, Yoza K and Häming L 2000 *J. Solid State Chem.* **151** 117
[26] Kim S-J, Hu S, Uher C, Hogan T, Huang B, Corbett J D and Kanatzidis M G 2000 *J. Solid State Chem.* **153** 321
[27] Shatruk M M, Kovnir K A, Lindsjö M, Presniakov I A, Kloo L A and Shevelkov A V 2001 *J. Solid State Chem.* **161** 233
[28] Blake N P, Latturner S, Bryan J D, Stucky G D and Metiu H 2001 *J. Chem. Phys.* **115** 8060
[29] Blake N P, Bryan D, Latturner S, Mollnitz L, Stucky G D and Metiu H 2001 *J. Chem. Phys.* **114** 10 063
[30] Kuznetsov V L, Kuznetsova L A, Kaliazin A E and Rowe D M 2000 *J. Appl. Phys.* **87** 7871
[31] Chakoumakos B C, Sales B C, Mandrus D G and Nolas G S 2000 *J. Alloys Compounds* **296** 80
[32] Meng J F, Charda Shekar N V, Badding J V and Nolas G S 2001 *J. Appl. Phys.* **89** 1730
[33] Iversen B, Bentien A, Palmqvist A E C, Bryan J D and Stucky G D 2000 *Proc. ICT2000 Conf. (Cardiff)*
[34] Rodriguez-Carvajal J 1992 'FULLPROF': a program for Rietveld refinement and pattern matching analysis *Physica* B **192** 55
[35] NONIUS KAPPA CCD package 1998 COLLECT, DENZO, SCALEPACK, SORTAV, Nonius Delft
[36] Sheldrick G M 1997 *SHELXS-97, Program for Crystal Structure Refinement* (University of Goettingen)
[37] Grytsiv A, Rogl P, Berger S, Paul C, Michor H, Bauer E, Hilscher G, Godart C, Knoll P, Musso M, Lottermoser W, Saccone A, Ferro R, Roisnel T and Noel H 2002 *J. Phys.: Condens. Matter* **14** 70
[38] Parthe E, Gelato L, Chabot B, Penzo M, Cenzual K and Gladyshevskii R 1568 *Typix Standardized Data and Crystal Chemical Characterization of Inorganic Structure Types* 8th edn (Berlin: Springer)
[39] Grytsiv A, Rogl P, Berger S, Paul C, Bauer E, Godart C, Ni B, Abd-Elmeguid M M, Saccone A, Ferro R and Kaczorowski D 2002 *Phys. Rev.* B at press